TUNNELING IN MANY-FERMION SYSTEMS*

John W. Negele

Center for Theoretical Physics
Laboratory for Nuclear Science
and Department of Physics
Massachusetts Institute of Technology
Cambridge, Massachusetts 02139 U.S.A.

Invited Talk Presented at
International Symposium on
MODERN DEVELOPMENTS IN NUCLEAR PHYSICS
Novosibirsk, U.S.S.R.
June 27 – July 1, 1987

Typeset in TEX by Roger L. Gilson

CTP #1491 July 1987

* This work is supported in part by funds provided by the U. S. Department of Energy (D.O.E.) under contract #DE-AC02-76ER03069.

TUNNELING IN MANY-FERMION SYSTEMS

John W. Negele

ABSTRACT

A microscopic theory of barrier penetration is presented in which the dynamical path is determined self-consistently. The essential roles of Fermion nodal surfaces and symmetry breaking are emphasized. The theory is applied to a solvable pedagogical model, which demonstrates its quantitative accuracy and the importance of solving for the optimal collective path. Similar features are observed in a more realistic calculation of a 32-Fermion system in three dimensions.

I. INTRODUCTION

The dynamics of self-bound many-Fermion systems poses a rich and challenging many-body problem. In this talk, I will address the microscopic theory of tunneling, which is applicable to a variety of nuclear phenomena ranging from spontaneous and induced fission to exotic radioactivity and heavy-ion fusion reactions. The techniques are quite general and are relevant to other many-Fermion systems as well, such as alkali metal clusters which display many features similar to nuclei.

A fundamental problem in formulating a microscopic theory of collective motion is to establish a general framework in which the Hamiltonian and the process specify the collective path. Physically, we expect some form of mean-field theory in which the optimal collective path through the classically forbidden region is determined self-consistently. From our experience with the Nilsson model and constrained Hartree–Fock calculations, we know that the rearrangement of the nodal structure of single-particle wave functions, and the associated symmetry breaking, will play a crucial role in the dynamics. This physical mean-field picture emerges simply and naturally from path integrals, which provide a powerful and convenient framework for a consistent quantum formulation of the problem. I will briefly review the general theory, details of which may be found in the literature,[1–3] and then address an illuminating pedagogical model and the fission of a nucleus in three dimensions.

II. MEAN FIELD THEORY

The physical foundation of mean-field theory is the idea that the behavior of each particle is governed by the mean field generated by interactions with all the other particles. This mean field, or equivalently, the one-body density matrix, is the obvious candidate to communicate collective information and we seek a formulation of the quantum many-body problem in which it emerges naturally. A path integral may be expressed in terms of evolution in any convenient complete or overcomplete set of states, and when evaluated in the stationary-phase approximation, yields a path in

this space. In this way, a many-body path integral in the space of Boson coherent states yields a self-consistent time-dependent Hartree theory, and a many-Fermion path integral in the space of Slater Determinants yields a time-dependent Hartree-Fock theory. To show the basic idea, I will first review the case of a path integral with a single degree of freedom, and then generalize to the many-body problem.

PATH INTEGRAL WITH A SINGLE DEGREE OF FREEDOM

A path integral deals with the non-commutativity of operators in quantum mechanics by expressing the evolution operator as a product of infinitesimal evolution operators for which non-commutativity may be ignored. Thus, one writes

$$\begin{aligned}\langle q_f|e^{-iHT}|q_i\rangle &= \langle q_f|e^{-i\epsilon H}\int dq_n|q_n\rangle\langle q_n|e^{-i\epsilon H}\int dq_{n-1}|q_n-1\rangle \\ &\times\langle q_{n-1}|e^{-i\epsilon H}\cdots\int dq_1|q_1\rangle\langle q_1|e^{-i\epsilon H}|q_i\rangle\end{aligned} \tag{2.1}$$

and

$$e^{-i\epsilon(T+V)} = e^{-i\epsilon T}\,e^{-i\epsilon V} + O(\epsilon^2)$$

with the result

$$\begin{aligned}e^{-iHT} &= \int D(q_1\cdots q_n)\; e^{i\epsilon\sum_k\left[\frac{m}{2}\left(\frac{q_{k+1}-q_k}{\epsilon}\right)^2 - V(q_k)\right]} \\ &\to \int D\left[q(t)\right]\, e^{i\int S(q(t))}\end{aligned} \tag{2.2}$$

where

$$S\left(q(t)\right) = \int_0^T dt\left[\frac{m}{2}\dot{q}(t)^2 - V\left(q(t)\right)\right]$$

is the classical action.

The eigenvalues of the one-dimensional potential sketched in (a) of Fig. 1 are obtained by calculating the poles of the resolvent

$$\begin{aligned}\mathrm{Tr}\,\frac{1}{E-H+i\eta} &= -i\int_0^\infty dT\, e^{iET}\int dq\langle q|e^{-iHT}|q\rangle \\ &= -i\int_0^\infty dT\, e^{iET}\int dq\int D\left[q(t)\right]\, e^{iS(q(t))}\end{aligned} \tag{2.3}$$

where it is understood that each trajectory $q(t)$ is periodic with end point q. The stationary-phase approximation is now applied in turn to each of the three integrals in (2.3). Variation of the trajectory $q(t)$ yields the Euler–Lagrange equations for the stationary solution

$$m\frac{d^2}{dt^2}q_0 = -\nabla(q_1) \tag{2.4}$$

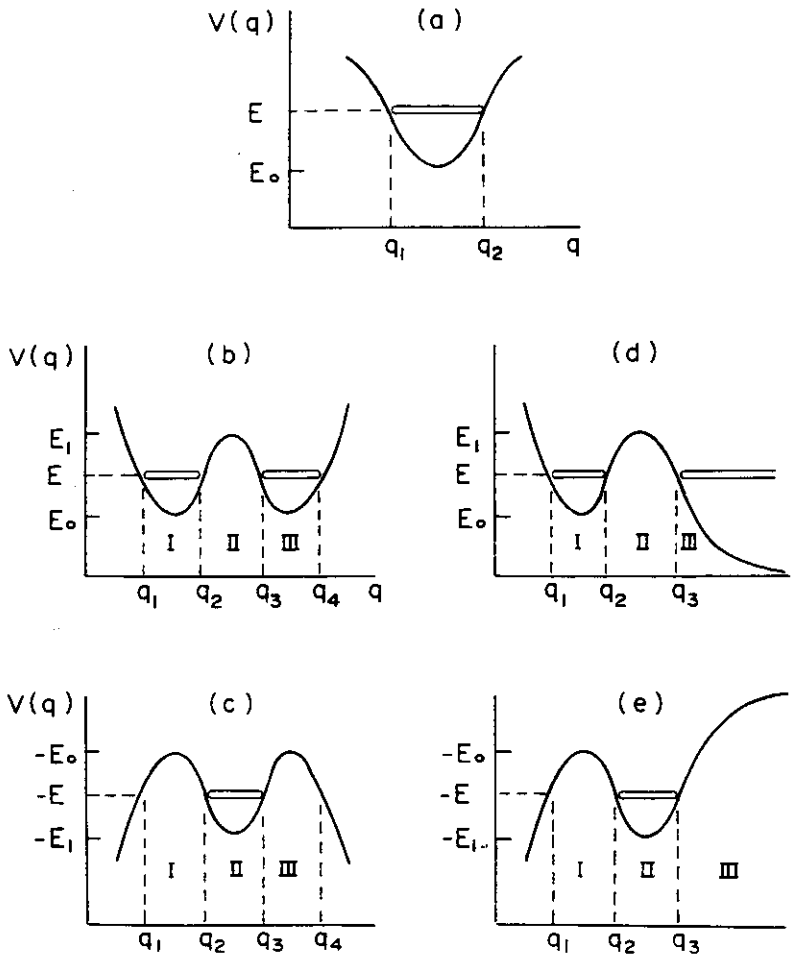

Fig. 1: Sketches of the potentials $V(q)$, periodic trajectories, and turning points as described in the text.

and variation of the endpoint yields conservation of p and thus $\dot{q}$ at the endpoint. Finally, stationarity with respect to T yields

$$E = -\frac{\partial S(q_0, T)}{\partial T} = E(T) \tag{2.5}$$

where $E(T)$ is the energy of a classical periodic orbit of period T

$$T(E) = \int_{q_1}^{q_2} \sqrt{\frac{m}{2\,(E - V(q))}}\, dq \ . \tag{2.6}$$

Summing over all multiples T_n of the fundamental period, we obtain

$$\mathrm{Tr}\,\frac{1}{E - H + i\eta} = A \sum_N f_n\, e^{iW(T_n)} \tag{2.7}$$

where

$$W(T_n) = ET_n + \int_0^{T_n} (p\dot{q} - H)\, dt = n \oint p\dot{q}$$

and A and f_n are factors arising from integrating quadratic fluctuations around the stationary points. Ignoring the factor f_n, the geometric series (2.7) yields poles for energies satisfying the quantization condition

$$\oint p\dot{q}\, dt = 2n\pi \tag{2.8}$$

for any integer n. Inclusion in f_n of the $\frac{\pi}{2}$ phase at each turning point replaces $2n\pi$ by the Bohr-Sommerfeld condition $(2n + 1)\pi$.

An interesting new feature arises in the analogous treatment of the double well in (b) of Fig. (1). In addition to periodic solutions of the form just discussed in regions I and III, there are stationary points in the complex T plane corresponding to periodic solutions in region II. A picturesque way to think of these solutions is to continue the classical equation of motion (2.4) to imaginary time by replacing (it) by τ, with the result

$$m\frac{d^2}{d\tau^2} q_0 = -\nabla\,(-V(q_0)) \tag{2.9}$$

That is, the trajectory which dominates the action in the stationary-phase sense corresponds to the classical solution in the inverted well. Such solutions were first introduced by Langer[6] in the context of bubble formation and correspond to the so-called instantons,[7,8] or bounces[9] in field theory. These trajectories give rise to the period

$$T_{\mathrm{II}}(E) = 2i \int_{q_2}^{q_3} \sqrt{\frac{m}{2\,(V(q) - E)}}\, dq \tag{2.10}$$

and a contribution to the trace of $e^{-W_{\mathrm{II}}}$, where

$$W_{\mathrm{II}} = 2 \int_{q_2}^{q_3} \sqrt{2m\,(V(q) - E)}\, dq \tag{2.11}$$

A general periodic trajectory in the double well, Fig. 1b, is composed of all possible combinations of periodic orbits in each of the three regions, giving rise to the multiple geometric series.

$$\begin{aligned}\mathrm{Tr}\,\frac{1}{E - H + i\eta} &= A \sum_{k\ell m} f_{k\ell m}\, e^{ikW_{\mathrm{I}}(E) - \ell W_{\mathrm{II}}(E) + imW_{\mathrm{III}}(E)} \\ &= \frac{-2e^{i(W_{\mathrm{I}} + W_{\mathrm{III}})} - e^{iW_{\mathrm{I}}} - e^{-W_{\mathrm{II}}} - e^{iW_{\mathrm{III}}}}{(1 + e^{iW_{\mathrm{I}}})\,(1 + e^{iW_{\mathrm{III}}}) + e^{-W_{\mathrm{II}}}}\end{aligned} \tag{2.12}$$

Expansion of the denominator and the relations $\frac{\partial W}{\partial E} = T(E) = \frac{1}{\omega}$ yield the familiar WKB energy splitting

$$E_n = E_n^0 \pm \frac{\omega}{2\pi}\, e^{-\frac{1}{2}W_{\mathrm{II}}} \tag{2.13}$$

The lifetime of a metastable state is obtained by distorting the right-hand well to extend to the edge of an arbitrarily large normalization box, yielding the potential sketched in Fig. 1d. The lifetime is obtained by evaluating the smoothed level density, defined as the imaginary part of Eq. (2.3) with the infinitesimal η replaced by a finite width γ, such that γ is smaller than any physical width but larger than the level spacing in the normalization box. In this case, we obtain periodic stationary solutions in region I as before, and in lowest approximation these yield the result Eq. (2.8) for the energies of the quasi-stable states. In addition, periodic imaginary-time trajectories are obtained in region II, corresponding to solution of the classical equations of motion in the inverted potential sketched in Fig. 1e. The role of periodic solutions in region III is quite different than for the double well, and one may show that $e^{iW_{III}}$ yields negligibly small contributions.

Thus, the smoothed density of states has poles at complex energies $E_n^0 + \Delta E_n$ satisfying $1 + e^{iW_I(E_n^0 + \Delta E_n)} = e^{-W_{II}(E_n^0 + \Delta E_n)}$ and expansion to first order in ΔE_n yields

$$\Delta E_n = -\frac{i\Gamma_n}{2} \tag{2.14}$$

where

$$\Gamma_n = 2\frac{\omega(E_n)}{2\pi}\, e^{-W_2(E_n)} \tag{2.14}$$

Near E_n, the level density is therefore proportional to $\left[(E - E_n)^2 + \left(\frac{\Gamma_n}{2}\right)^2\right]^{-1}$ so that Γ_n is the inverse lifetime of the metastable state. To within the factor of 2 which is presumably corrected by a careful evaluation of all corrections to the stationary-phase approximation, Eq. (2.14) is recognized as the familiar WKB formula for tunneling decay of a metastable state.

This simple example from one-dimensional quantum mechanics turns out to embody all the essential features of our subsequent treatment of the eigenstates of large-amplitude collective motion and tunneling decay of quantum many-body systems.

MANY PARTICLES

There are many alternative functional integrals for many-particle systems, each with its own advantages and limitations. The present objective is to obtain mean-field physics in the stationary-phase approximation. Hence, the many-particle Feynman path integral is inappropriate, since it leads yields the classical equations of motion. Rather, we will use overcomplete sets of coherent states and Slater determinants, respectively, for Bosons and Fermions.

The essential idea is most simply displayed for Bosons. Using coherent states $|\phi\rangle = e^{\int d\vec{x}\phi(\vec{x})\hat{\psi}^\dagger(\vec{x})}|0\rangle$ and inserting the completeness relation

$$\int \mathcal{D}[\phi^*(\vec{x}),\phi(\vec{x})]\, e^{-\int dx\,\phi^*(\vec{x})\phi(\vec{x})}|\phi\rangle\langle\phi| = 1 \tag{2.15}$$

between each factor $e^{-\epsilon H}$ in the evolution operator, we obtain[1]

$$\langle\phi_f|e^{-iHT}|\phi_i\rangle = \int \mathcal{D}\left[\phi^*(\vec{x},t),\phi(\vec{x},t)\right]\, e^{iS(\phi^*,\phi)} \tag{2.16}$$

where

$$\begin{aligned} S(\phi^*,\phi) = &\int_0^T dt \int d\vec{x}\,\phi^*(\vec{x},t) \\ &\times\left[-\frac{d}{dt}+\frac{\nabla^2}{2m}-\frac{1}{2}\int d\vec{x}\,\phi^*(\vec{x},t)\phi(\vec{x},t)v(\vec{x}-\vec{x})\right]\phi(\vec{x},t) \end{aligned} \tag{2.17}$$

plus a boundary term which is not relevant to the present discussion. The action, (2.17), is of the Hartree form and $\phi(x,t)$ has the physical interpretation of the condensate wave function. If we make the stationary-phase approximation and represent the evolution operator by a single optimal stationary trajectory, we obtain the time-dependent Hartree equation for the condensate wave function

$$i\frac{\partial}{\partial t}\phi(\vec{x},t) = \left[-\frac{\nabla^2}{2m}+\int d\vec{x}'\,\phi^*(\vec{x}',t)\phi(\vec{x}',t)v(\vec{x}-\vec{x}')\right]\phi(\vec{x},t) \tag{2.18}$$

This equation describes the evolution of a drop of liquid ^{4}He in terms of a simple classical, function $\phi(\vec{x},t)$, which for low energy phenomena is nodeless. Although we have not stressed it, all the physics associated with short-range correlations, including the "hole" the repulsive core of the Helium-Helium potential punches in the relative wave function, is subsumed in an effective interaction v. If one could attach repulsive charges of arbitrary strength to each Helium atom, one could generate a fission problem free of any of the Fermion nodal physics familiar in the nuclear case, and the bounce solution would smoothly evolve from a single Helium drop to two separated fragments.

The analogous result for Fermions is obtained economically using the completeness relation in the space of Slater determinants

$$\begin{aligned} \prod_{k,j}\int \mathcal{D}\left[\phi_k^*(\vec{x})\phi_j(\vec{x})\right]\delta\left(\int d\vec{x}\phi_k^*(\vec{x})\phi_j(\vec{x})-\delta_{kj}\right) \\ \times\mathcal{N}|\phi_1\phi_2\cdots\phi_N\rangle\langle\phi_1\phi_2\cdots\phi_N| = 1 \end{aligned} \tag{2.19}$$

where $|\phi_1\phi_2\cdots\phi_N\rangle$ denotes a Slater determinant composed of single-particle functions $\phi_1\cdots\phi_N$ and $\mathcal{N}$ is an irrelevant normalization factor.[1,10] The evolution operator becomes

$$\begin{aligned} \langle\Phi_f|e^{-iHT}|\Phi_i\rangle = &\int \mathcal{D}\left[\phi_1^*\cdots\phi_N^*\phi_1\cdots\phi_N\right]\prod_{kj} \\ &\times\delta\left(\int dx\,\phi_k^*(\vec{x},t)\phi_j(\vec{x},t)-\delta_{kj}\right)e^{iS(\phi^*\phi)} \end{aligned} \tag{2.20}$$

where the action is

$$S(\phi^*\phi) = \int_0^T dt\left[\int dx\sum_k \phi_k^*(\vec{x},t)i\frac{d}{dt}\phi(\vec{x},t)-\mathcal{H}(\phi^*,\phi)\right] \tag{2.21}$$

and the Hartree Fock energy functional is defined

$$\begin{aligned} \mathcal{H}(\phi^*,\phi) = &\sum_k\int d\vec{x}\phi_k^*(x)\frac{-\nabla^2}{2m}\phi_k(x) \\ &+\frac{1}{2}\sum_{k,j}\int d\vec{x}\,d\vec{x}'\Big[\phi_k^*(\vec{x},t)\phi_j^*(\vec{x}',t)v(\vec{x}-\vec{x}') \\ &\times\left\{\phi_k(\vec{x},t)\phi_j(\vec{x}',t)-\phi_k(\vec{x}',t)\phi_j(\vec{x},t)\right\}\Big]\ . \end{aligned} \tag{2.22}$$

Note that the action (2.21) has the form of a classical field theory[11] with conjugate variables $i\phi_k^*$ and ϕ_k

$$\frac{\partial}{\partial t}\phi_k = \frac{\partial\mathcal{H}}{\partial(i\phi_k^*)} \qquad \frac{\partial}{\partial t}(i\phi_k^*) = -\frac{\partial\mathcal{H}}{\partial\phi_k} \tag{2.23}$$

so that we might naively expect the results for one degree of freedom to be generalized with $q\to\phi_k$, $p\to i\phi_k^*$.

Application of the stationary-phase approximation to $S(\phi^*\phi)$ with the orthonormality constraint in (2.20) enforced by Lagrange multipliers yields the following four-dimensional generalization of the usual three-dimensional Hartree-Fock problem

$$\left[i\frac{\partial}{\partial t}+\frac{\nabla^2}{2m}-\int d\vec{x}'\sum_k\phi_k^*(\vec{x}',t)\phi_k(\vec{x}',t)v(\vec{x},\vec{x}')+\text{exch}\right]\phi_j(\vec{x},t) = \lambda_j\phi_j(\vec{x},t) \tag{2.24}$$

with the boundary conditions that the $\phi_k(\vec{x},t)$ vanish on the spatial boundary and are periodic with period T. Evaluating Eq. (2.20) using the periodic solutions to Eq. (2.24) yields the stationary phase result

$$Tr\frac{1}{E-H+i\varsigma}\propto\int_0^\infty dT\ e^{i[ET+S(T)]}\equiv\int_0^\infty dT\ e^{iW(T)} \tag{2.25}$$

where $S(T)$ is the action $S[\phi*,\phi]$, Eq. (2.21), evaluated with the periodic solutions of period T. The stationary-phase approximation to the T integral in Eq. (2.25) is performed precisely as in Eq. (2.17) for the one-dimensional problem, with the result that

$$Tr\frac{1}{E-H+i\varsigma} \approx \frac{e^{iW(T_0)}}{1-e^{iW(T_0)}} \tag{2.26}$$

yielding the quantization condition

$$W(T_0)=\sum_k i\int dx\int_0^T dt\phi_k^*(x,t)\frac{\partial}{\partial t}\phi_k(x,t)=n2\pi \tag{2.27}$$

As expected, this quantization condition has the structure of (2.8), with q,p replaced by $i\phi_k^*$ and ϕ_k.

The problem of barrier penetration can also be treated analogously to the one-dimensional example in section 3.1. The first step is to continue from real time to imaginary time. As before, we let $it\rightarrow\tau$ and it is convenient to use a symmetric time interval $(T/2,\ -T/2)$. One then finds[3] that the single-particle wave function $\phi_k(\vec{x},t)\rightarrow\tilde{\phi}_k(\vec{x},\tau)\equiv\phi_k(\vec{x},t=\frac{\tau}{i})$ which is purely real. The proper identification of the adjoint wave functions for analytic continuation is $\phi_k(\vec{x},t^*)^*\rightarrow\tilde{\phi}_k(\vec{x}-\tau)$. Note that the replacement $\phi^*(t)\phi(t)$ by $\tilde{\phi}(-\tau)\phi(\tau)$ systematically incorporates necessary physical properties, such as maintaining normalization of the density, and cancelling time-dependent factors of the form $\tilde{\phi}_k(\vec{x},\tau)=e^{\lambda\tau}\phi_k(x)$.

The action, Eq. (2.21), thus becomes

$$\begin{aligned}\tilde{S}[\tilde{\phi}(-\tau),\tilde{\phi}(\tau)]=\int d\tau\Bigg[&\int d\vec{x}\sum_k\tilde{\phi}_k(\vec{x},-\tau)\Big[-\frac{\partial}{\partial\tau}+\frac{\nabla^2}{2m}\Big]\tilde{\phi}_k(\vec{x},\tau)\\&-\frac{1}{2}\int\int d\vec{x}d\vec{x}'\tilde{\phi}_k(\vec{x},-\tau)\tilde{\phi}_j(\vec{x}',-\tau)v(\vec{x}-\vec{x}')\\&\times\{\tilde{\phi}_k(\vec{x},\tau)\tilde{\phi}_j(\vec{x}',\tau)-\tilde{\phi}_k(\vec{x}',\tau)\tilde{\phi}_j(\vec{x},\tau)\}\Bigg]\end{aligned} \tag{2.28}$$

To see the analog to the inverted potential (2.9) it is useful to transform from the conjugate variables ϕ^* and ϕ to time-even and time-odd variables which correspond to coordinates and moments. We will seek to express the problem in the general form of a Lagrangian with a position-dependent mass[12]:

$$L=\frac{1}{2}M(Q)\ \dot{Q}^2-V(Q) \tag{2.29a}$$

so that

$$P=\frac{\partial L}{\partial\dot{Q}}=M(Q)\ \dot{Q} \tag{2.29b}$$

$$H=P\dot{Q}-L=\frac{P^2}{2M(Q)}+V(Q) \tag{2.29c}$$

and thus

$$L=P\dot{Q}-P\frac{1}{2M(Q)}P-V(Q) \tag{2.29d}$$

Now, consider the real time action (2.21), neglecting exchange terms for convenience, and change variables[3] such that

$$\phi_k(\vec{x},t)=\sqrt{\rho_k(\vec{x},t)}e^{i\chi_k(\vec{x},t)} \tag{3.20}$$

where $\rho(\vec{x},t)=\rho(\vec{x},-t)$ and $\chi(\vec{x},t)=-\chi(\vec{x},-t)$. Then, the action may be written

$$\begin{aligned}S&=\int dt\left[i\sum_k\phi_k^*\dot{\phi}_k-\mathcal{H}(\phi_k^*,\phi_k)\right]\\&=\int dt\int d\vec{x}\sum_k\left[\chi_k\frac{\partial}{\partial t}\rho_k-\frac{1}{2m}\rho_k(\nabla\chi_k)^2\right]-V(\rho_k)\end{aligned} \tag{2.31}$$

where

$$V(\rho_k)=H\Big(\sqrt{\rho_k},\sqrt{\rho_k}\Big)$$

that is, $V(\rho_k)$ is the Hartree-Fock energy functional Eq. (2.5) with a time-even determinant composed of real wave functions $\sqrt{\rho_k}$. The form of Eq. 2.31) is completely analogous to Eq. (2.29) where χ_k corresponds a to momentum, ρ_k corresponds to a coordinate, $\overleftarrow{\nabla}\frac{\rho}{2m}\overrightarrow{\nabla}$ is the inverse coordinate - dependent mass parameter and the potential is given by the HF energy functional.

In the imaginary-time case,the appropriate change of variables is

$$\tilde{\phi}_k(\vec{x},\tau)=\sqrt{\tilde{\rho}_k(\vec{x},\tau)}\,e^{-\tilde{\chi}_k(\vec{x},\tau)} \tag{2.32}$$

where

$$\tilde{\rho}_k(\vec{x},\tau)\equiv\rho_k\left(\vec{x},t=\frac{\tau}{i}\right)=\tilde{\rho}_k(\vec{x},-\tau)$$

and

$$\tilde{\chi}_k(\vec{x},\tau)=-i\chi_k\left(\vec{x},t=\frac{\tau}{i}\right)=\tilde{\chi}_k(\vec{x},-\tau)$$

In this case, the action is

$$\tilde{S}=-\int d\tau\left(\int d\vec{x}\sum_k\left[\tilde{\chi}_k\frac{\partial}{\partial\tau}\tilde{\rho}_k-\frac{1}{2m}\tilde{\rho}_k\left(\nabla\tilde{\chi}_k\right)^2\right]+V(\rho_k)\right) \tag{2.32}$$

Comparing Eqs. (2.31) and (2.32) we see that relative to the terms involving χ, $V(\rho)$ undergoes a relative sign change, so that the stationary solutions simply correspond to solution in the inverted potential $V(\rho)$. Note that $V(\rho)$ is the multidimensional HF energy surface, the properties of which are known essentially only through constrained HF calculations.

In one respect, the problem of spontaneous decay in many dimension differs essentially from that in one dimension. Whereas in Fig. 1 parts d and e there was no problem in joining the solutions in the classically allowed and forbidden regions at the classical turning point, to obtain the geometric series, Eq. (3.23), in the multi-dimensional case the complete wave function composed of single-particle functions $\phi_\kappa(\tau,t)$ and $\tilde{\phi}_\kappa(\tau,t)$ must be joined at the classical turning point. Whereas this joining can in fact be demonstrated at the HF minimum, it does not occur in general and one must, therefore, use the alternative dilute instanton gas approximation[1,4,13] to evaluate the premultiplying factor corresponding to $\frac{\omega}{2\pi}$ in Eq. (2.14). With this one deficiency, repetition of the steps leading to Eq. (3.27) yields the following result for the lifetime of a metastable state

$$\Gamma = \sum_c \lim_{T\to\infty} \Gamma^c(T) \tag{2.33a}$$

as a sum of particle widths

$$\Gamma^c(T) = K\ e^{-\int_{-\tau/2}^{T/2} d\tau \int d\vec{x} \sum_k \tilde{\phi}_k^c(\vec{x},-\tau)\frac{\partial}{\partial\tau}\tilde{\phi}_k^c(\vec{x},\tau)} \tag{2.33b}$$

where $\tilde{\phi}_k^c$ represents a periodic solutions to Eq. (3.90) for each distinct fission channel c

$$\left[\frac{\partial}{\partial\tau} - \frac{\nabla^2}{2m} + \int d\vec{x}' \sum_k \tilde{\phi}_k(x',\tau)\tilde{\phi}_k(x',\tau)v(\vec{x}-\vec{x}')\right]\tilde{\phi}_j(\vec{x},\tau) = \lambda_j\tilde{\phi}_j(\vec{x},\tau) \tag{2.33c}$$

SYMMETRY BREAKING

The truly novel feature of the many-Fermion tunneling problem which sets it apart from familiar problems in field theory is the physics associated with the nodal structure of the wave functions. The bounce solutions entering into vacuum decay and instantons in gauge theory are bosonic and smoothly evolve between classically allowed domains. In contrast, the nodal structure of Fermionic wave functions must rearrange substantially, and accounts for much of the richness of the physics.

The simplest case is in one spatial dimension. The bounce solution to a simple model with four orbitals described in Ref. [2] is shown in Fig. 2. Whereas the density evolves smoothly through the barrier, the nodes of each of the individual single-particle wave functions are substantially rearranged. At the initial time, the wave functions are simply the zero-, one-, two-, and three-node eigenfunctions of the static HF potential. The elongation to form a neck at the origin at $\tau = 0$ changes the structure, so that the first two wave functions resemble even and odd combinations of nodeless wave functions localized on separate sides of the origin and the last two correspond to even and odd combinations of wave functions located on each side of the origin containing a single node. Hence, a more illuminating representation would be states corresponding to sums and differences of the first two and last two wave functions, in which the total wave function would approximately factorize into two nearly separated subsystems.

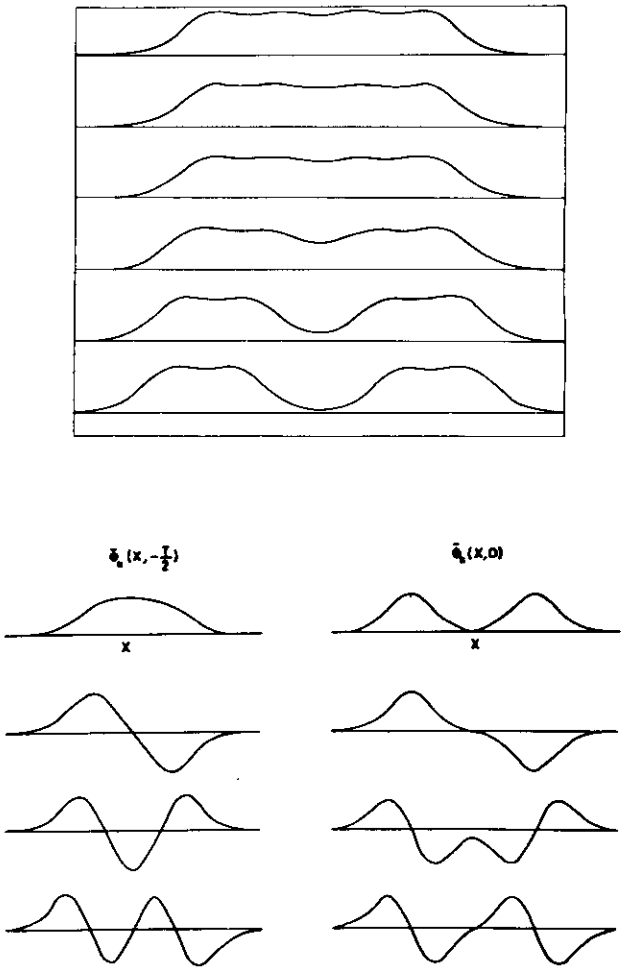

Fig. 2: Density profiles and single-particle wave functions for the imaginary-time mean-field solution for the fission of a 16-particle system in one-dimension. The density profiles are shown at evenly-spaced time intervals from $\tau = -T/2$ to $\tau = 0$, and the wave functions are shown at $\tau = -T/2$ and $\tau = 0$.

In higher dimensions, as the shape of the mean field changes, the relative energies of wave functions with different numbers of nodes in the wide and narrow directions change, and the theory must address the corresponding level crossings.

To be specific, consider a deformed harmonic oscillator potential with the s and p orbital filled to produce a ^{16}O core. As the potential is elongated in the z-direction, an unoccupied state ϕ_{002} with two nodes in the z-direction decreases in energy while the occupied state ϕ_{100} with one node in the x-direction increases in energy, and at some point these levels cross. If the self-consistent field is constrained to be axially and reflection symmetric, these two levels cross without mixing. One possibility is to introduce pairing, in which case the mean field retains its symmetries, the orbitals contribute to the density in the form $a^2|\phi_{100}|^2 + b^2|\phi_{002}|^2$ and the pairing interaction governs the dynamics of tunneling. The other possibility is to allow the mean field to break all symmetries. In this case, near the level crossing the single-particle wave function is some mixture of the two orbitals, the orbitals contribute to the density in the form $|a\phi_{100} + b\phi_{002}|^2$ and the self-consistent broken symmetry mean field governs the dynamics. Before exploring this symmetry breaking in a three-dimensional system, it is illuminating to examine a simple solvable model.

III. A PEDAGOGICAL MODEL

To study this mean field symmetry breaking in barrier penetration, G. Bertsch, G. Puddu, P. Arve and I have constructed a simple solvable model which exhibits the essential features.[14] For motivation, we consider a Hartree-like Hamiltonian for a large number of particles which could be in either of two single-particle states of a two-dimensional well: ϕ_x with a node in the x-direction and ϕ_y with a node in the y-direction. Further, we let z_i characterize the deformation of the orbital containing the i^{th} particle. As the single-particle well is elongated in the x-direction, the z_i-increase, the single-particle energy of ϕ_x decreases, and the energy of ϕ_y increases. Since there are only two states in the model, and we are characterizing the deformation of each orbital by the variable z_i, each particle may be represented by the coordinate z_i and a spin. The full Hamiltonian for N distinguishable particles is

$$H = \sum_{i=1}^{N} \left(-\frac{1}{2}\frac{d^2}{dz^2} + \frac{1}{2}z^2 \right)_i + \kappa \left(\sum_{i=1}^{N} z_i \right) \left(\sum_{i=1}^{N} \sigma_z(i) \right) + \lambda \left(\sum_{i=1}^{N} \sigma_x(i) \right)^2 . \quad (3.1)$$

The second term represents the dependence of the single-particle energies on the total deformation of the system. The last term is the two-body residual interaction, representing the fact that for either a δ-function interaction or a separable interaction of the form $\sum_i x_i y_i \sum_j x_j y_j$ the following two-body matrix elements are roughly equal $\langle \phi_x \phi_x | v | \phi_x \phi_x \rangle = \langle \phi_x \phi_x | v | \phi_x \phi_x \rangle$. Note that by transforming to collective c.m. variables $z = \sum_{i=1}^{N} z_i$ and $(N-1)$ relative coordinates, the relative coordinates decouple and one has a single dynamical variable coupled to the total spin. In this sense, the model may be viewed as a generalization of the familiar Lipkin model extended to allow for barrier penetration.[15]

When $\lambda = 0$, the total spin projection $M = \langle \sum_i \sigma_z(i) \rangle$ is a good quantum number, the Hamiltonian is a shifted harmonic oscillator, the wave function is a shifted

oscillator state $\phi_i(z, M, \nu) \propto H_\nu \left(\frac{1}{\sqrt{N}}(z - \kappa MN) \right) e^{-\frac{1}{2N}(z-\kappa MN)^2} |M\rangle$, and there are two degenerate ground states: all spin up at $z = \kappa NM$ and all spin down at $z = -\kappa NM$. For non-zero λ, the diagonal matrix elements of the shifted oscillators are supplemented by off-diagonal matrix elements connecting $|M-2, \nu\rangle$ with $|M+2, \nu'\rangle$, the two degenerate ground states are split by tunneling, and the exact solution may be obtained by numerical matrix diagonalization.

The parameters appropriate to nuclear fission have been determined to reproduce a single-particle frequency corresponding to a giant quadrupole frequency of 10 – 15 MeV, a barrier height of 5 MeV and mixing comparable to that obtained in fission with realistic residual interaction matrix elements of the order of 0.2 MeV. Because all N level crossings occur simultaneously, an additional factor of N occurs in the mixing due to coherence, and the strength of the residual interaction has been reduced accordingly. The sign of λ is important in the Hartree solution, and the physical choice is negative λ, corresponding to an attractive residual interaction. The final parameters we use are $N = 40$, $\kappa = 0.00603$ and $\lambda = -0.0005$.

It is instructive to compare two approximations to the exact ground state splitting: the conventional cranking model based on constrained Hartree-Fock solutions and the imaginary time-dependent mean-field approximation derived in the previous section. By the proof of Eq. (6.15) of Ref. [2], one may show that the stationary-phase approximation corresponds to an expansion in $\frac{1}{N}$ for this model and thus should be extremely accurate.

The static mean field solution is obtained in the usual way using a product of single-particle wave functions of the form $\phi_i = \phi(z_i)\binom{\cos\frac{\theta}{2}}{\sin\frac{\theta}{2}}$. Variation yields the single-particle Hamiltonian

$$H_{sp} = -\frac{1}{2}\frac{d^2}{dz^2} + \frac{1}{2}z^2 + \kappa\langle\sigma_z\rangle z + \kappa\langle z\rangle\sigma_z + 2\lambda\langle\sigma_x\rangle\sigma_x + fz \quad (3.2)$$

where f is a constraining field used to constrain $\langle z \rangle$ and $\phi(z)$ is a shifted oscillator. The expectation values of the spin operators in the wave function are $\langle\sigma_x\rangle = N\cos\theta$ and $\langle\sigma_x\rangle = N\sin\theta$, so that $\langle\sigma_x\rangle$ may be expressed in terms of $\langle\sigma_z\rangle$. From the coefficients of σ_x and σ_z in the single-particle Hamiltonian, we conclude that either $\langle\sigma_x\rangle = 0$, in which case all spins are either up or down and there is no symmetry breaking, or else $\langle\sigma_x\rangle = \frac{\kappa\langle z\rangle}{2\lambda}$, corresponding to mixing of the two spin states and symmetry breaking. Using these relations, the energy and $\langle\sigma_x\rangle$ may be expressed as functions of $\langle z\rangle$, with the results shown in Figs. 3 and 4. The salient feature is that when the collective variable $\langle z \rangle$ is constrained, the system retains its symmetry for much of the path. Only close to the level crossing is the symmetry broken with a significant expectation value $\langle\sigma_x\rangle \neq 0$. As derived in Ref. [14], the collective energy and cranking inertia in the symmetric regime are

$$E(\langle z\rangle) = \frac{N}{2} + \frac{\langle z\rangle^2}{2N} - \kappa|\langle z\rangle|N \quad (3.3a)$$
$$I = \kappa^2 N^3$$

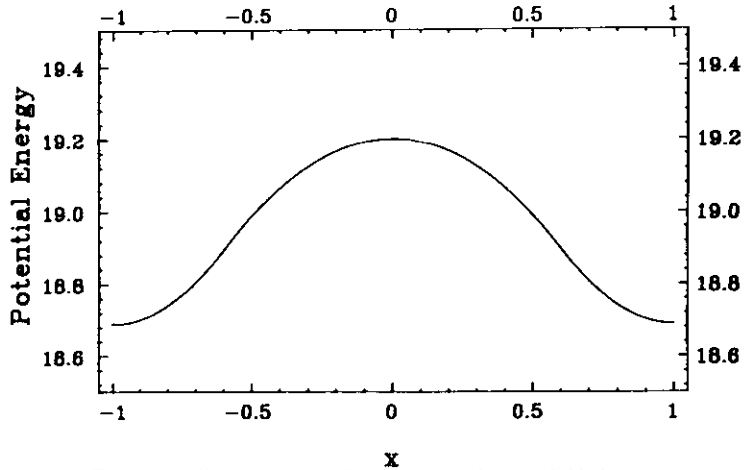

Fig. 3: Collective potential in constrained mean-field theory.

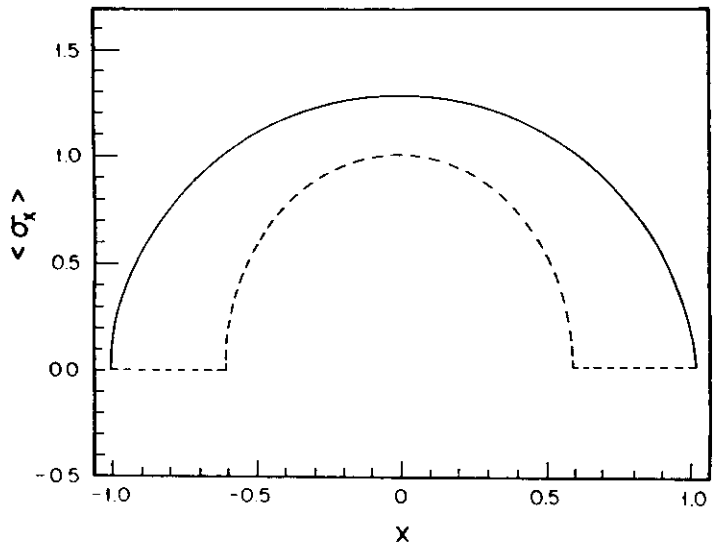

Fig. 4: Collective motion path for the spin model in constrained mean-field (dashed line) and in imaginary time mean-field theory (solid line).

and in the broken symmetry regime are

$$E(\langle z\rangle) = \frac{N}{2} + \frac{1}{2}\left(\frac{1}{N} - \frac{\kappa^2}{2|\lambda|}\right)\langle z\rangle^2 + \lambda N^2$$
$$I(\langle z\rangle) = \kappa^2 N^3 - \frac{1}{8\lambda N\left(\frac{4\lambda^2}{\kappa^4 N^2} - \frac{\langle z\rangle^2}{\kappa^2 N^4}\right)} \qquad (3.3b)$$

from which the level splitting may be evaluated analytically in the WKB approximation.

The energy splitting in the imaginary-time mean-field theory is given by

$$\Delta E = \frac{\omega}{\pi} e^{-\frac{N}{2}\int_{-\mathcal{T}/2}^{\mathcal{T}/2} d\tau \langle\phi(-\tau)|\frac{\partial}{\partial\tau}|\phi(\tau)\rangle} \qquad (3.4a)$$

where the wave function ϕ is the solution to

$$\left[\frac{\partial}{\partial\tau} - \frac{1}{2}\frac{\partial^2}{\partial z^2} + \frac{1}{2}z^2 + \kappa\langle\sigma_z\rangle_\tau z + \kappa\langle z\rangle_\tau\sigma_z + 2\lambda\langle\sigma_x\rangle_\tau\sigma_x\right]\phi(z,\tau) = \epsilon\phi(z,\tau) \qquad (3.4b)$$

with periodic boundary conditions and $\langle\mathcal{O}\rangle_\tau \equiv \langle\phi(-\tau)|\mathcal{O}|\phi(\tau)\rangle$.

Whereas the penetrability is well-defined and straightforwardly calculable for any energy, the pre-multiplying factor in Eq. 3.4a is more difficult. For the ground state, it is unambiguously defined as the ratio of two determinants in the dilute instanton gas approximation[9] and should be well-approximated by the collective frequency ω in the outer well. We have thus used this oscillator frequency for all energies. As the energy is increased, it is clear physically that other degrees of freedom play increasingly important roles, so this prescription will systematically overestimate the splitting.

The self-consistent path defined by the solution to (3.4b) is shown by the dashed line in Fig. 4. Note that in contrast to the constrained case, $\langle\sigma_z\rangle$ is non-zero for the entire trajectory, so that the symmetry is broken for the whole optimal trajectory. In this model, we can improve the static constrained theory appreciably[14] by constraining $\langle\sigma_z\rangle$ instead of $\langle z\rangle$, which generates a path much closer to the optimal path. This constraint effectively grabs hold of the relevant level-crossing degree of freedom from the start. In a realistic fission calculation, however, there is no way to constrain the corresponding single-particle degrees of freedom, so one must necessarily constrain a collective deformation variable analogous to z.

The difference between the optimal path and the static constrained path is dramatically demonstrated by the approximations obtained for level splittings below the barrier. For the ground state, splitting $\Delta E = e^{-12.96}$, the imaginary-time mean field yields $e^{-13.02}$ whereas the constrained mean field yields $e^{-19.5}$. The corresponding results for excited states are graphed in Fig. 5.

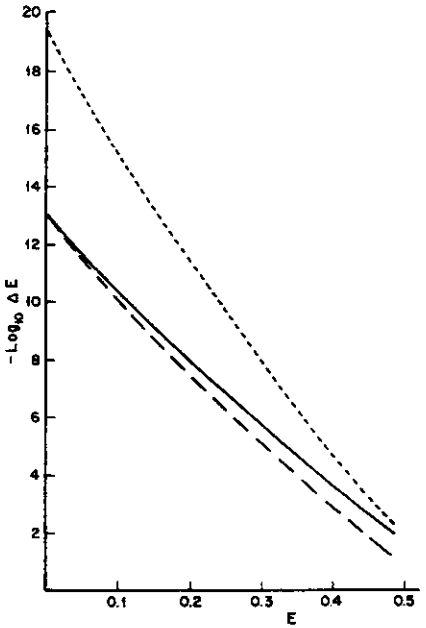

Fig. 5: Comparison of exact splittings as a function of energy (solid curve) with the imaginary-time mean-field theory (dashed lines) and constrained mean-field theory (dotted lines).

IV. FISSION OF ^{32}S IN THREE DIMENSIONS

Finally, I will show the results of a calculation with G. Puddu and R. Wolff[16] which displays symmetry breaking associated with orbital rearrangement in a nucleus in three dimensions. We calculate the symmetric fission of ^{32}S using a density-dependent interaction with the strength of the Coulomb force increased to produce fission. The collective variable analogous to $\langle z \rangle$ in the previous model is the quadrupole moment, and the total energy and single particle energies in a constrained Hartree Fock calculation are shown in Figs. 6 and 7. The eighth orbital is the last occupied state and changes from having two nodes in the transverse direction at small deformation to having three nodes in the longitudinal direction at large deformation.

The time-dependent mean field equations are solved as follows.[17] We begin by solving the imaginary-time analog of the RPA equations at the top of the barrier shown in Fig. 6, with a constraint on the time average of the quadrupole moment to render the calculation stable. The period is then successively increased, and for each period the eigenvalue problem (2.33c) is solved iteratively. Since the largest eigenvalue of the evolution operator $e^{-\int_{-T/2}^{T/2} h_{sp}(\tau)d\tau}$ corresponds to the lowest occupied state

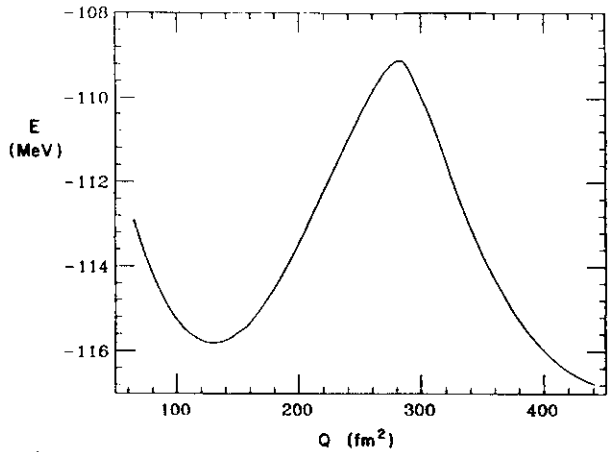

Fig. 6: Hartree-Fock energy as a function of deformation $\langle Q \rangle$.

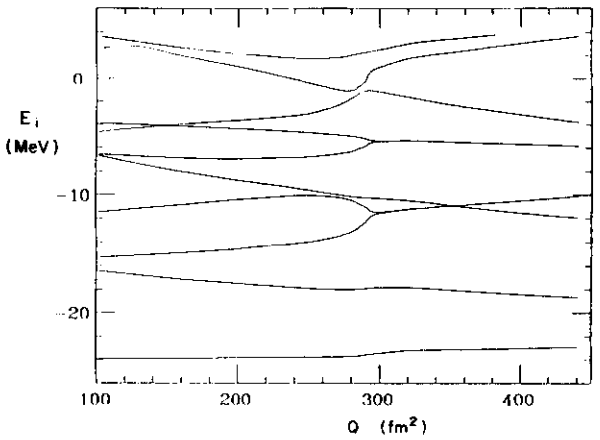

Fig. 7: Single-particle energies as a function of deformation $\langle Q \rangle$. The lowest eight orbitals are occupied.

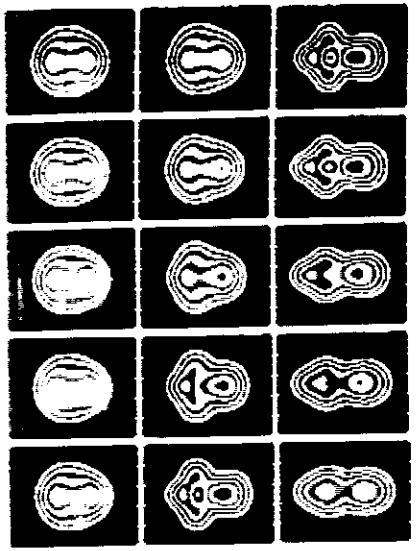

Fig. 8: Contour plots at sequential times of the density integrated over z

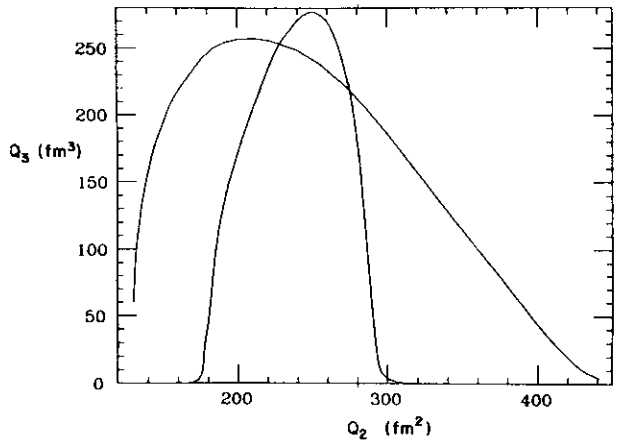

Fig. 9: Collective motion path for the fission of ^{23}S in constrained mean-field theory (dashed line) and in imaginary-time mean-field theory (solid line).

ϕ_1 $(-T/2)$, successive application of the evolution operator to an arbitrary state converges to ϕ_1. Higher states are calculated by application of the evolution operator and orthogonalization to all lower states. In this way, the eigenstates $\left\{\phi_i^{(n+1)}\right\}$ in the potential generated by $\left\{\phi_i^{(n)}\right\}$ are calculated and iterated to self-consistency. As T is increased, the solution approaches the bounce solution to any desired accuracy.

The sequence of shapes through which the nucleus evolves in shown in Fig. 8. The salient feature is the significant symmetry breaking throughout the entire evolution through the barrier, and it is clear that nodal rearrangement is playing a significant role in the dynamics. The similarity between this calculation and the pedagogical model of the last section may be seen by expressing the trajectory by the quadrupole moment Q_2, which characterizes the collective deformation and corresponds to $\langle z^2 \rangle$, and the octupole moment, Q_3, which characterizes the symmetry breaking and corresponds to $\langle \sigma_x \rangle$. The paths for the solution of the imaginary-time mean-field theory and for static mean-field theory with a quadrupole constraint are shown in Fig. 9. The similarity to the paths in Fig. 4 for the spin model is striking. Again the symmetry is broken along the entire optimal path, whereas the symmetry breaking is restricted to a small domain in the immediate vicinity of the level crossing in the constrained theory. Hence, as in the case of the spin model, solving the equations for the optimal path is expected to provide a major quantitative improvement in the theory.

In summary, the quantum mean-field theory which arises naturally from path integrals, self-consistently specifies the optimal collective path, and incorporates the basic physics of nodal rearrangement. It thus provides a microscopic understanding of many key elements of collective dynamics in many-Fermion systems.

REFERENCES

1. J. W. Negele and H. Orland, *Quantum Many-Particle Systems* (Addison–Wesley, Reading, MA, 1987).
2. J. W. Negele, *Rev. Mod. Phys.* **54** (1982) 947.
3. S. Levit, J. Negele and Z. Paltiel, *Phys. Rev.* **C21** (1980) 1603; **C22** (1980) 1979.
4. H. Reinhardt, *Nucl. Phys.* **A367** (1981) 269.
5. H. Kleinert, *Phys. Lett.* **B69** (1977) 9.
6. J. Langer, *Ann. Phys.* (New York) **54** (1969) 258.
7. A. M. Polyakov, *Nucl. Phys.* **B121** (1977) 429.
8. G. 't Hooft, *Phys. Rev. Lett.* **37** (1976) 8.
9. S. Coleman, *Phys. Rev.* **D15** (1977) 2929.
10. J. P. Blaizot and H. Orland, *Phys. Rev.* **C24** (1981) 1740.
11. A. K. Kerman and S. E. Koonin, *Ann. Phys.* (New York) **100** (1976) 332.
12. H. Tang and J. W. Negele, *Nucl. Phys.* **A406** (1983) 205.

13. J. W. Negele, "Nuclear Structure and Heavy Ion Collisions," Varenna Summer School LXXVII (*Soc. Italiana di Fisica*, Bologna, Italy, 1979).

14. P. Arve, G. F. Bertsch, J. W. Negele and G. Puddu, MIT preprint CTP #1484 (1987).

15. H. Lipkin, N. Meshkov and A. Glick, *Nucl. Phys.* **62** (1965) 188.

16. R. Wolff, G. Puddu and J. W. Negele, to be published.

17. G. Puddu and J. Negele, *Phys. Rev.* **C35** (1987) 1007.